Journal of Alloys and Compounds 509 (2011) 8632–8640

Contents lists available at ScienceDirect

Journal of Alloys and Compounds

journal homepage: www.elsevier.com/locate/jallcom

Effect of Mg, Si and Cu content on the microstructure of dilute 6000 series aluminium alloys

Aiza Jaafar[a,*], Azmi Rahmat[b], Zuhailawati Hussain[a], Ismail Zainol[c]

[a] School of Materials and Mineral Resources Engineering, Universiti Sains Malaysia, 14300 Nibong Tebal, Penang, Malaysia
[b] School of Materials Engineering, Universiti Malaysia Perlis, Taman Muhibah, 02600 Jejawi, Arau Perlis, Malaysia
[c] Chemistry Department, Faculty of Science and Mathematics, Universiti Pendidikan Sultan Idris, 35900 Tanjung Malim, Perak, Malaysia

ARTICLE INFO

Article history:
Received 18 February 2010
Received in revised form 13 May 2011
Accepted 16 May 2011
Available online 7 June 2011

Keywords:
Metal and alloys
Precipitation
Microstructure
TEM

ABSTRACT

The effect of Mg, Si and Cu content on the microstructural development during ageing treatment of dilute 6000 series alloys have been investigated using transmission electron microscopy (TEM). Four dilute alloys were used in this study. These alloys were subjected to quenching and artificial ageing at 100 °C, 185 °C and 300 °C. The microstructural developments of the precipitates formed were monitored by TEM. The ageing temperature of 100 °C was found to be too low to form precipitates. It was found that needle or rod-shaped precipitates were formed in the alloys after ageing at 185 and 300 °C. Prolong ageing up to 1000 h at 300 °C resulted in the formation of Mg_2Si precipitate that coexists with the type of AlFeSi and Si precipitates. The results show a correlation between the Mg_2Si, Si and Cu content on the microstructure of the four dilute alloys after ageing treatment.

1. Introduction

Al–Mg–Si alloys or 6000 series alloys are widely used for medium strength structural applications and also in increasing demand in the automotive industry. These alloys have been the materials of choice for skin panels because they have a combination of good formability and medium strength. The alloys are age hardenable and strengthened by Mg_2Si, which is the primary hardening phase. These alloys often require precipitation hardening through heat treatment in order to develop their optimum mechanical properties.

Numerous investigations on the effect of alloy composition on the microstructure and mechanical properties of the aged alloys have been carried out [1–4]. Silicon additions in excess (ExSi) of that required to form Mg_2Si has a significant effect on the precipitation hardening response [4]. Small addition of Cu to the alloys is known to refine and increase the precipitation density of Mg_2Si precipitates [3]. The presence of Mn and Cr has been reported to modify the microstructures and improves the mechanical properties such as toughness and ductility of the alloys [5].

Although the precipitation hardening process of 6000 series alloys has been extensively studied by many workers [6–9] but the understanding of the precipitation hardening process and its sequence is very complex and still remains controversial. The precipitation hardening process is difficult to optimise because it is governed by many parameters such as in addition to alloy composition, solution treatment temperature, time between quenching and ageing, ageing time and temperature, which could affect the precipitation hardening behaviour [7,10]. The precipitation sequence of Al–Mg–Si alloys, which has been generally accepted in the literature, is the following [6,11,12]:

$$\alpha_{SSSS} \rightarrow \text{GP zones} \rightarrow \beta'' \text{ needle-shaped precipitates} \rightarrow \beta' \text{ rod-shaped precipitates} \rightarrow \beta\, Mg_2Si \text{ precipitates}$$

where α (SSSS) is supersaturated solid solution and GP zones are the precursor of the β″ needle-shaped precipitates. It has been reported by many authors that the β″ needle-shaped precipitates is very important because it may play a major role as an effective strengthening precipitate in the 6000 series alloys [4,6,7]. Ageing at higher temperatures will finally bring the equilibrium of β-precipitate or Mg_2Si phase, formed as platelets, lying in the $(1\,0\,0)_{Al}$ planes [13].

The precipitation hardening process in the dilute 6000 series alloys is still new and not many works has been reported. The aim of the present study is to investigate the effects of Mg, Si and Cu content on the precipitation hardening behaviour and the microstructural development during artificial ageing of some dilute 6000 series aluminium alloys. This alloy has a potential to be used in the automotive industry because it is economical due to less amount of alloying addition used.

* Corresponding author. Tel.: +60 5 4583492.
E-mail addresses: cnaizza@gmail.com, cnaiza.gd07@student.usm.my (A. Jaafar).

0925-8388/$ – see front matter © 2011 Elsevier B.V. All rights reserved.
doi:10.1016/j.jallcom.2011.05.061

Table 1
Chemical composition of the alloys (wt%).

	Alloy	Si	Fe	Cu	Mn	Mg	Ti	Mg_2Si	ExSi
Cu-containing	A1	0.22	0.17	0.1	0.03	0.20	0.01	0.32	0.1
	A2	0.79	0.17	0.1	0.03	0.51	0.01	0.80	0.5
Cu-free	B1	0.20	0.17	0.001	0.03	0.20	0.01	0.32	0.08
	B2	0.76	0.17	0.002	0.03	0.50	0.01	0.79	0.47

2. Experimental procedure

The composition of the 6000 series dilute alloys is given in Table 1. They are divided into two groups: Cu-containing and Cu-free alloys, which consist of the more dilute alloys (A1 and B1) and the less dilute alloys (A2 and B2).

These alloys are in extruded form with 40 mm wide and 3 mm thick. The extruded alloys were cold rolled to 1.5 mm thickness. After cold rolling, the alloys were solution treated at 530 ± 5 °C for 5 min and quenched into cold water. The quenched alloys were then artificially aged at 100 °C, 185 °C and 300 °C with a specific ageing time. TEM analysis was performed on the alloys which have been aged at 100 °C for 1000 h, 185 °C for 30 h and for artificially aged alloys at 300 °C, the alloys were concentrated on three ageing times: 3 min, 1 h and 1000 h. The aged alloys samples were punched into 3 mm diameter discs. The discs were ground to a thickness of between 100 and 200 μm using silicon carbide paper of 1200 grit. The disc were then electropolished in a solution of 70% methanol and 30% nitric acid cooled to -30 ± 1 °C using a Struers Tenupol-3 jet electropolisher operating at a potential difference of 9 V. The Philips EM400 and CM200 operating at 120 kV and 200 kV, respectively were used to observe the microstructures and to obtain selected area diffraction (SAD) pattern. Samples were orientated with the electron beam in the [1 0 0] directions of the matrix. The Philips CM200 and Tecnai 20 operating at 200 kV were used for EDX analysis. Thickness measurement was made using convergent beam electron diffraction pattern technique [14]. The length and the number of precipitates were measured and counted from TEM micrographs. The density of the precipitates was calculated by dividing the number of measured precipitates by the volume of field [15].

3. Results and discussion

The strengthening of 6000 series alloys is dependent upon the type, morphology, orientation, distribution, number density and the size of precipitates [16]. Figs. 1–5, 7 and 8 show bright-field (BF) TEM micrographs representing the typical microstructure of both Cu-containing and Cu-free alloys that have been artificially aged at 100 °C, 185 °C and 300 °C, respectively. All the TEM micrographs

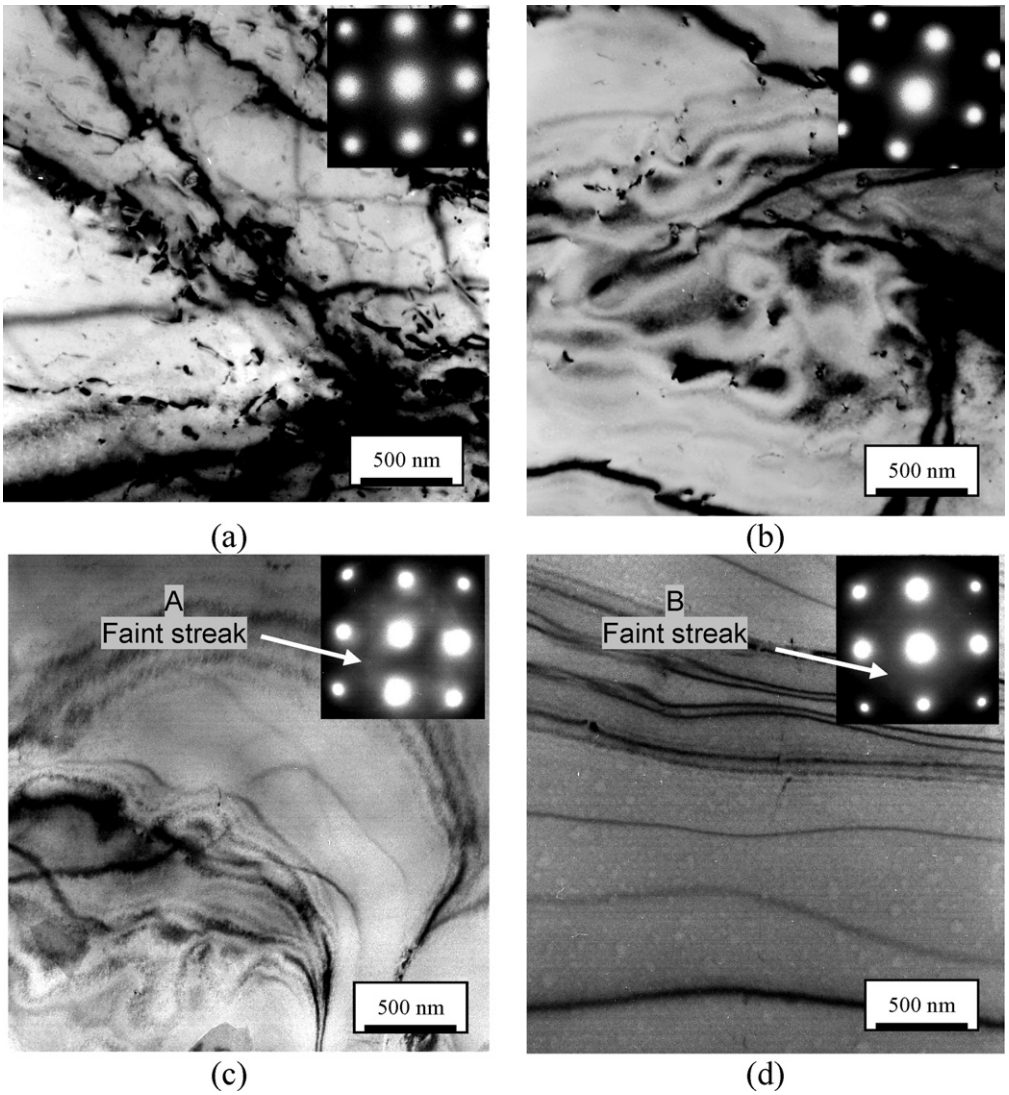

Fig. 1. TEM micrographs and corresponding SAD pattern (inset) of alloys aged at 100 °C for 1000 h. Electron beam is in the [1 0 0] matrix direction. (a) Alloy A1, (b) Alloy B1, (c) Alloy A2 and (d) Alloy B2. Arrows A and B showing faint streak in SAD patterns of alloys A2 and B2 and it can be clearly seen on the computer screen.

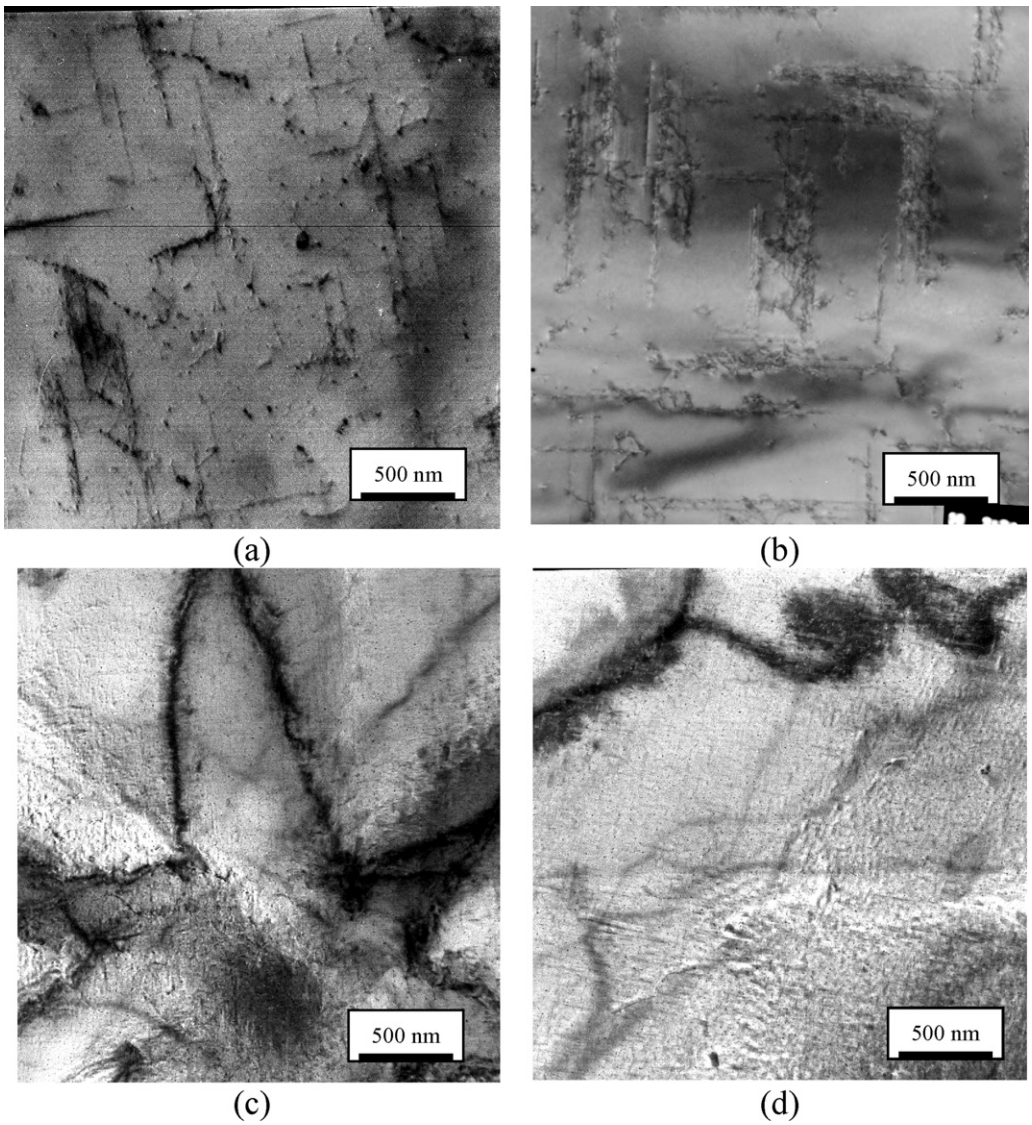

Fig. 2. TEM micrographs of alloys aged at 185 °C for 30 h. Electron beam is in the [1 0 0] matrix direction. (a) Alloy A1, (b) Alloy B1, (c) Alloy A2 and (d) Alloy B2. At this stage, fine needle-shaped precipitates predominate in the less dilute alloys.

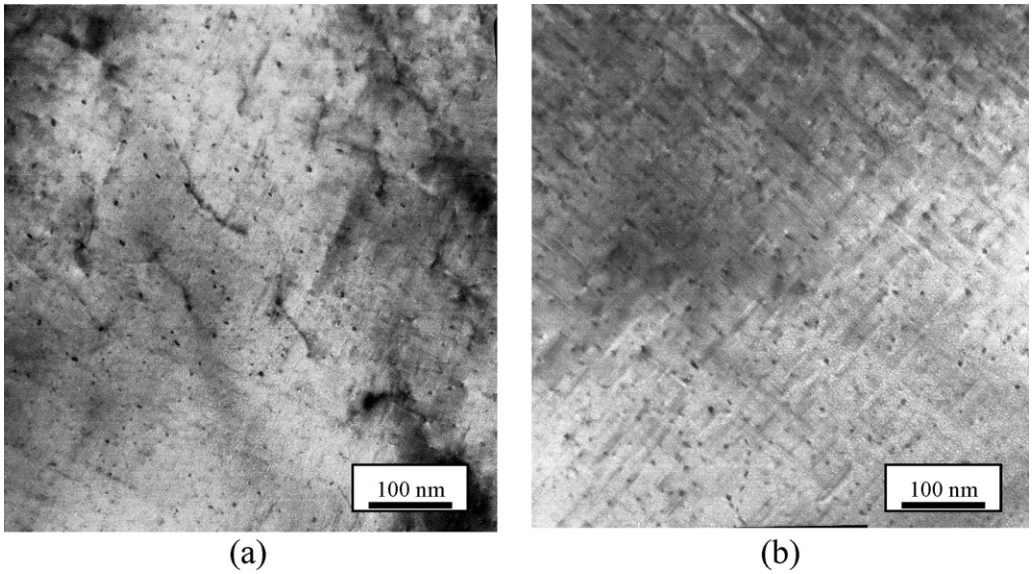

Fig. 3. TEM micrographs of (a) Alloy A2 and (b) Alloy B2 aged at 185 °C for 30 h (taken at higher magnification). Electron beam is in the [1 0 0] matrix direction. The needle-shaped precipitates are clearly observed in the less dilute alloys.

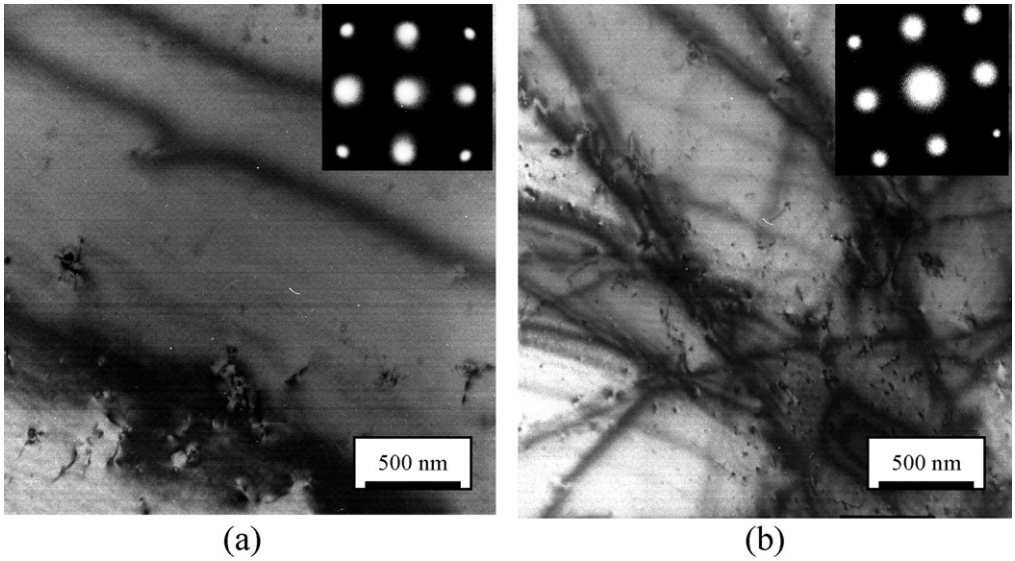

Fig. 4. TEM micrographs and corresponding SAD pattern (inset) of (a) Alloy A1 and (b) Alloy B1 aged at 300 °C for 3 min. Electron beam is in the [1 0 0] matrix direction.

are with the incident electron beam in the [1 0 0] direction of the matrix.

3.1. Ageing for 1000 h at 100 °C

Fig. 1 shows the TEM bright field micrographs and corresponding SAD pattern of all dilute alloys, which have been aged at 100 °C for 1000 h. It can be seen that no distinct features of precipitates were observed in the more (Fig. 1a and b) and less dilute alloys (Fig. 1c and d) at the low ageing of 100 °C. The results also show that no faint streak pattern was found in SAD pattern of the more dilute alloys (A1 and B1) but it was observed in the less dilute alloys (A2 and B2). The presence of faint streaks on SAD pattern proposes that there is precipitate in the less dilute alloys. The faint streaks were usually generated from precipitates parallel to the beam direction. These observations suggest that the precipitates may be fully coherent with the matrix and their size is too small, therefore these precipitates are not clearly resolved under TEM microscope used in this study. The method to identify the nature of precipitation based on the formation of streak pattern co-exist with diffraction spot of aluminium was also used by Yassar and Field [9], Dutta and Allen [12] and Murayama et al. [17].

Based on the TEM results, it is proposed that the precipitates might have been formed at different rates where the precipitation kinetics might be slightly different in the more and less dilute alloys. The driving force for the nucleation of precipitates is high at low ageing temperature but the diffusion process is slow; therefore the precipitate distribution is now dominated by the slow growth. At low ageing temperature, the precipitates need a very long time to grow and become large. Therefore in precipitation sequence of the alloys, the transformation process from small precipitates into intermediate precipitates, as well as into equilibrium precipitates is very slow. The presence of faint streak on SAD pattern of the less dilute alloys suggests that the precipitation kinetics in the less dilute alloys is significantly faster than in the more dilute alloys.

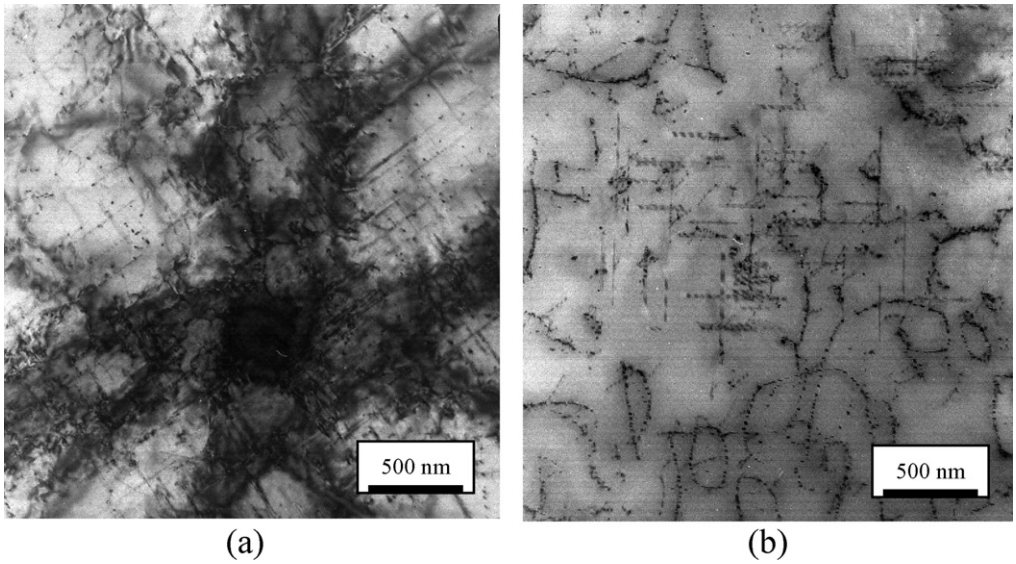

Fig. 5. TEM micrographs of (a) Alloy A2 and (b) Alloy B2 aged at 300 °C for 3 min. Electron beam is in the [1 0 0] matrix direction. At this stage, needle-shaped precipitates predominate in the less dilute alloys.

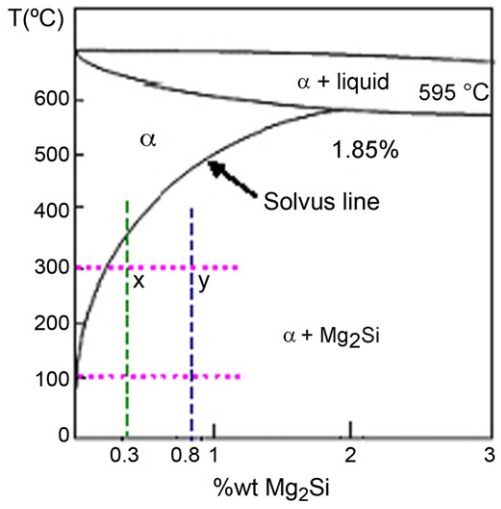

Fig. 6. The pseudo-binary Al and Mg_2Si phase diagram.

Table 2
The number density and average length of needle-shaped precipitates observed by TEM after ageing at 185 °C for 30 min.

Alloy	Number density ($\times 10^{13}$ cm^{-3})	Length (nm)
A1	6.67	790 ± 41
B1	5.56	937 ± 73
A2	455.29	269 ± 14
B2	353.04	273 ± 19

3.2. Ageing for 30 h at 185 °C

Fig. 2 shows the TEM bright field micrographs obtained from all dilute alloys aged for 30 h at 185 °C. It is very interesting to notice that ageing at 185 °C for 30 h produced a microstructure consisting of large amount of needle-shaped precipitates. These precipitates are dominant in the microstructure and they are responsible to give rise to the maximum strength of 6000 series alloys in the T6-condition [6,18].

The number density and length of needle-shaped precipitates after ageing at 185 °C for 30 min are summarised in Table 2. Among the four dilute alloys, the highest number densities of the precipitates were found in the less dilute alloys. The precipitates in alloys A2 and B2 were smaller in size and therefore they are more densely

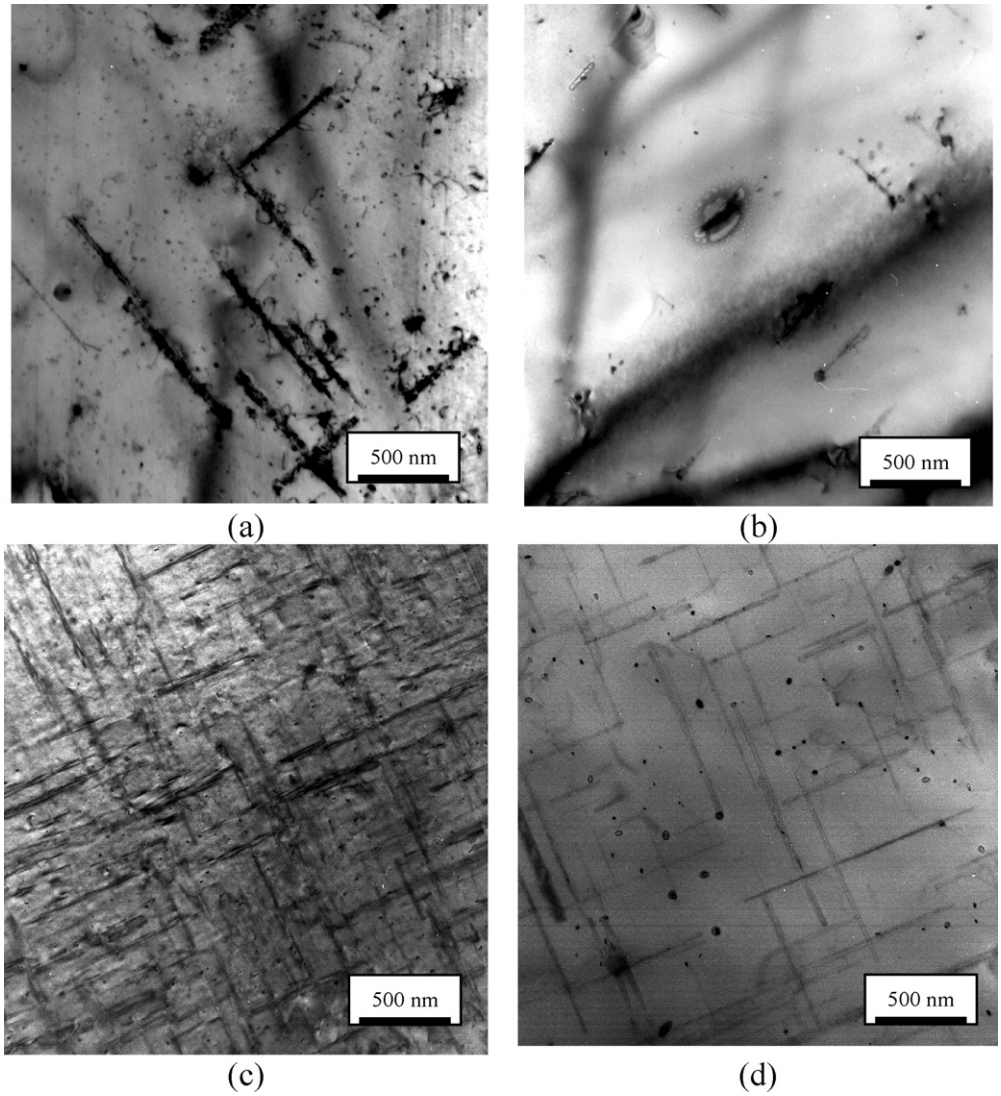

Fig. 7. TEM micrographs of alloys aged at 300 °C for 1 h. Electron beam is in the [1 0 0] matrix direction. (a) Alloy A1, (b) Alloy B1, (c) Alloy A2 and (d) Alloy B2. At this stage, further coarsened needle-shaped precipitates predominate in the less dilute alloys.

Table 3
The number density and average length of needle or rod-shaped precipitates after ageing at 300 °C for 3 min, 1 h and 1000 h.

Alloy	300 °C (3 min)		300 °C (1 h)		300 °C (1000 h)	
	Number density ($\times 10^{13}$ cm^{-3})	Length (nm)	Number density ($\times 10^{13}$ cm^{-3})	Length (nm)	Number density ($\times 10^{13}$ cm^{-3})	Length (nm)
A1	–	–	1.67	818 ± 75	–	–
B1	–	–	1.24	360 ± 38	–	–
A2	28.22	485 ± 76	34.02	601 ± 70	0.86	2289 ± 38
B2	10.87	517 ± 94	11.90	947 ± 81	–	–

dispersed and closely spaced than those observed in alloys A1 and B1. This observation can be clearly seen in the TEM micrographs of microstructure at high magnification (Fig. 3a and b), which shows that the precipitates were fine, dense and homogeneously distributed throughout the matrix. From these results, it appears that the higher Mg_2Si and ExSi contents level in these alloys give a higher number density of precipitates than that of the more dilute alloys. Similar observation was also reported by Gupta et al. [4]) when they studied precipitation hardening in Al–Mg–Si alloys. They found that a higher volume fraction and refined distribution of precipitates increased with increasing Mg_2Si and ExSi contents.

However, as presented in Table 2, alloy A2 from Cu-containing alloys shows the highest number density of precipitates than alloy B2 from Cu-free alloys. This observation suggests that the combination of higher ExSi (0.5 wt%) and Cu (0.1 wt%) contents in the alloy would increase the number density of the precipitates. The role of ExSi in 6000 series alloys is not only enhancing the ageing response but it also increases the solvus temperature of Mg_2Si which in turn increases the thermodynamic driving force for precipitation during ageing [19]. Alloys with a constant Mg_2Si content after quenching from the solution treatment temperature should be more supersaturated with the higher ExSi. The enhanced driving force increases the number of nucleation sites and results in an increasing a finer distribution of needle-shaped precipitates [19].

The higher number density of precipitates in alloy A2 also suggests that the addition of Cu provides favourable nucleation sites for the precipitates formation. Cu refines the precipitates and increasing the density of their precipitation [3]. In addition, an increase of

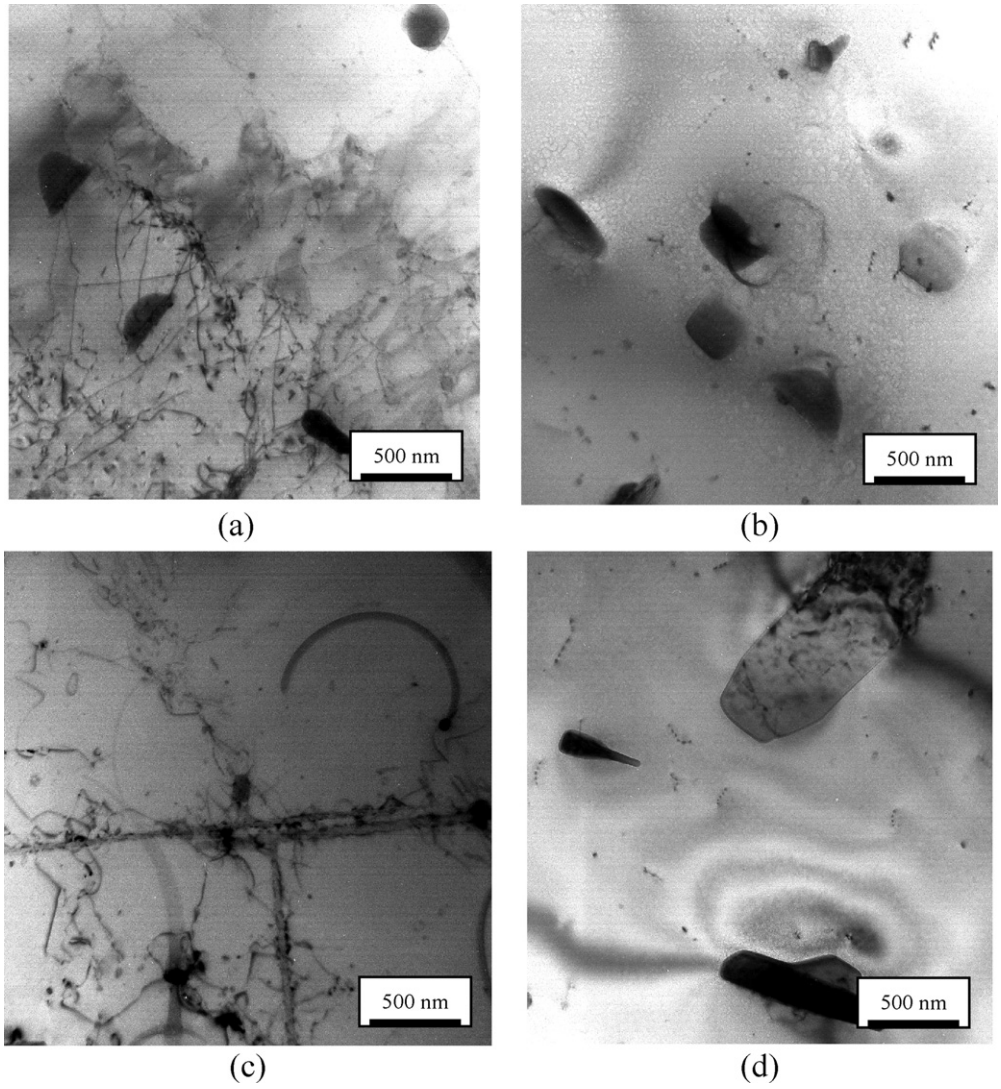

Fig. 8. TEM micrographs of alloys aged at 300 °C for 1000 h. Electron beam is in the [1 0 0] matrix direction. (a) Alloy A1, (b) Alloy B1, (c) Alloy A2 and (d) Alloy B2.

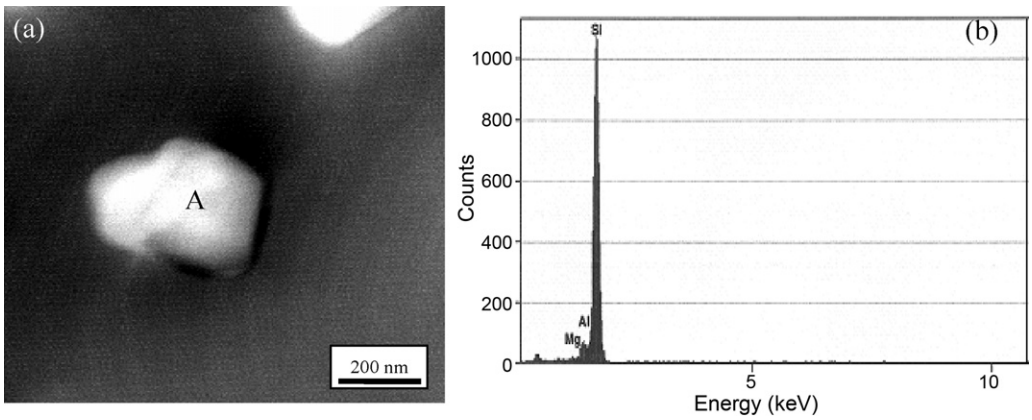

Fig. 9. (a) TEM dark field micrographs of alloy B2 after ageing at 300 °C for 1000 h and (b) EDX spectrum from coarse precipitate labelled A.

number density of precipitates and ageing response of the alloy A2 are probably attributed to the formation of Q phase or lath-shape precipitates in the alloy. Basically, the lath-shaped precipitates existed in the Al–Mg–Si–Cu alloys system and normally they were appeared at peak aged and/or during overageing [20,21]. The presence of high number density of all those precipitates may effectively stop the dislocation movement resulting an increase in ageing response of the alloys [22,23]. From these results, it can be seen that the precipitation hardening kinetics was also enhanced by the addition of 0.1 wt% Cu.

The number density of precipitates in alloys A1 and B1 were found to be similar. However alloy B1, which forms precipitates mainly on dislocations, shows the lowest number density of precipitates among the dilute alloys in line with the low solute contents of ExSi and Cu. It can be seen that the length of needle-shaped precipitates for alloy A1 is shorter than alloy B1. This proves that addition of small Cu refines the precipitate microstructure of the alloys which in turn increases the number density of precipitates. The same observation was also made by Tamizifar and Lorimer [2], who reported the effect of Cu resulting in refinement of the precipitates in alloy 6061. This further supported by Laughlin and Miao [1] who found that the microstructure of the high Cu alloy of 6022 was much finer than that of the lower Cu alloy.

3.3. Ageing at 300 °C

In order to study the changes in the precipitation state during ageing at high temperature (300 °C) by TEM, three ageing times of 3 min, 1 h and 1000 h were chosen. Figs. 4, 5, 7 and 8 present the bright-field (BF) TEM micrographs of the alloys artificially aged for 3 min, 1 h and 1000 h at 300 °C, respectively. As the ageing time progressed from 3 min to 1000 h, the growth of precipitates were observed clearly in all dilute alloys.

3.3.1. Ageing for 3 min at 300 °C

Fig. 4 shows bright field micrographs and the corresponding SAD patterns of the more dilute alloys ageing at 300 °C for 3 min while Fig. 5 shows bright field micrographs of the less dilute alloys ageing at the same condition.

At the relatively high ageing temperature of 300 °C, precipitates were expected to form in all the more and less dilute alloys. However, there is no evidence of precipitates formation was detected in neither the micrograph nor diffraction patterns in the more dilute alloys for the short ageing time, 3 min at 300 °C (Fig. 4). Nevertheless, the needle-shaped precipitates were clearly visible on the bright-field micrographs for the less dilute alloys (Fig. 5).

At high ageing temperature, the driving force for precipitation is low, but the diffusion and growth of precipitates are very fast. Therefore, precipitation becomes dominated by nucleation. When the alloy is aged to the higher ageing temperature, there may be a delay before nucleation occurs but once nucleation does occur, the precipitates will grow very fast.

In 6000 series alloys, it is believed that the delay before nucleation of precipitates is dependent on the alloy composition. This can be explained by using phase diagram as shown in Fig. 6. In the more dilute alloys, the Mg_2Si compositions (0.32 wt%) are closer to the solvus line (point *x*). Therefore, alloys A1 and B1 have a lower driving force and low probability for nucleating precipitates. Based

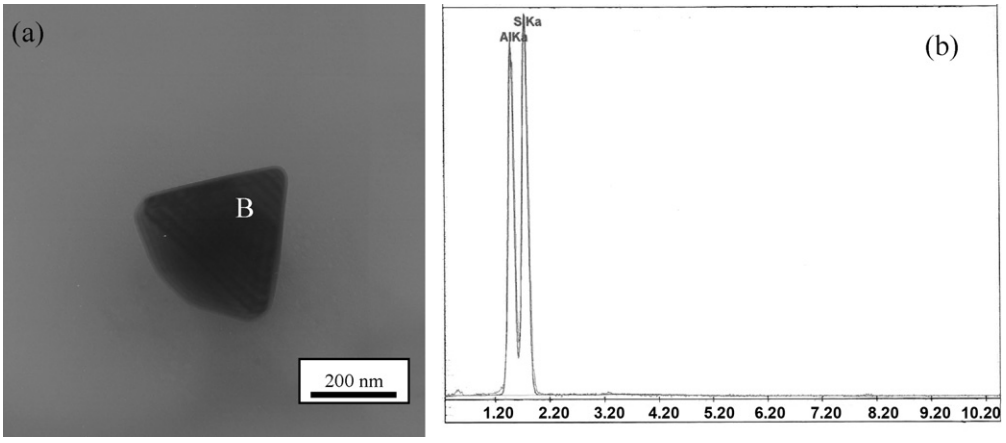

Fig. 10. (a) TEM bright field micrographs of alloy B2 after ageing at 300 °C for 1000 h and (b) EDX spectrum from coarse precipitate labelled B.

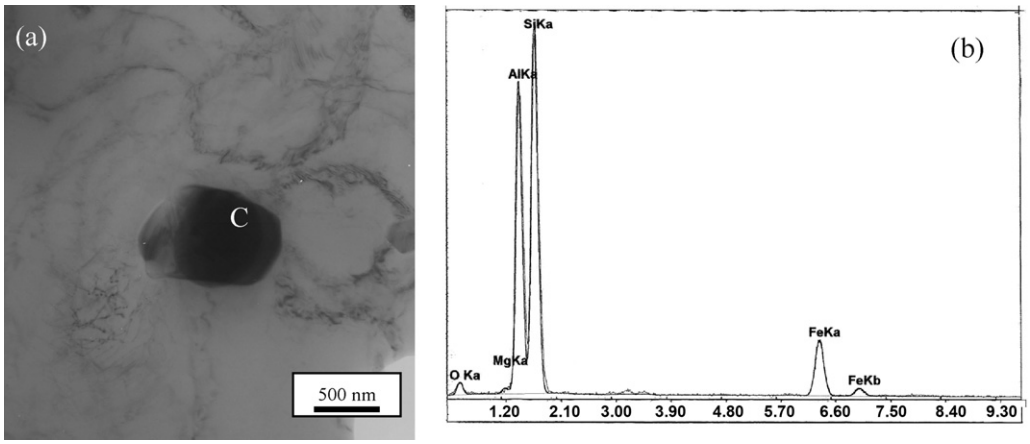

Fig. 11. (a) TEM bright field micrographs of alloy B2 after ageing at 300 °C for 1000 h and (b) EDX spectrum from coarse precipitate labelled C.

on this study, it is proposed that the precipitation kinetics in the more dilute alloys is significantly delayed for the short ageing time at high ageing temperature.

Alloys A2 and B2, which the Mg_2Si composition (~0.8 wt%) is far from the solvus line, have a high driving force and a high probability to form precipitates (point *y*). From TEM results, it can be inferred that the rate of precipitate formation is very fast in the less dilute alloys compared to the more dilute alloys.

Table 3 shows the number density and length of needle or rod-shaped precipitates after ageing at 300 °C for 3 min, 1 h and 1000 h. As observed from Table 3 the number density of precipitates in alloy A2 is higher than that of alloy B2. The results presented above show that the higher solute content of ExSi (0.50 wt%) and Cu (0.1 wt%) in alloy A2 led to increasing the precipitates density in the microstructure of the alloy. The presence of Cu refines the precipitates microstructure, thus the density of precipitates in the alloy A2 is higher compared to alloy B2. These results also suggest that the kinetics of precipitation in the alloy A2 from Cu-containing alloys appear to be faster than that in B2 from Cu-free alloys. However, the average length of the needle-shaped precipitates in alloys A2 and B2 is similar. This result infers that the length of precipitates is not significant for the less dilute alloys at high ageing temperature of 300 °C for shorter ageing time.

3.3.2. Ageing for 1 h at 300 °C

The microstructure development for alloys aged at 300 °C for 1 h is shown in Fig. 7. After ageing for 1 h, needle-shaped precipitates were appeared in the more dilute alloys meanwhile the precipitate became coarsened in the less dilute alloys.

The number density of the precipitates follows the similar pattern as shown in alloys artificially aged at 185 °C for 30 h but has much lower number density. From Table 3, it is interesting to note that alloy B1, which is the more dilute Cu-free alloy shows the shortest and lowest number density of precipitates than other alloys. This is in line with the fact that alloy B1 has low amount of ExSi and Cu contents, thus produce lower number density of precipitates than other alloys. From the TEM results, it is inferred that the alloys with higher Mg_2Si and ExSi contents with or without Cu (A2 and B2) produced higher number density of precipitates than other alloys. This result is consistent with the observation found in alloys aged at 185 °C for 30 h.

Generally, it can be seen that the length of precipitates in dilute alloys increases with increasing ageing temperature from 185 °C to 300 °C. By increasing ageing temperature, the precipitates formation is accelerated and the growth of precipitates is increased. This can be clearly seen in TEM micrographs where longer and larger sized of the precipitates are revealed at the higher ageing temperature compared to the lower ageing temperature (Figs. 2, 5, 7 and 8c).

3.3.3. Ageing for 1000 h at 300 °C

There is a distinct difference between the microstructures of alloys that aged for 3 min, 1 h and 1000 h at 300 °C as shown in Figs. 4, 5, 7 and 8 respectively. When the alloy is over-aged, the precipitates will dissolve and a number of coarser precipitate particles will be formed [18]. In the present study, prolonging the ageing time up to 1000 h resulted in the formation of rod-shaped and coarse precipitates with different morphologies, as shown in Fig. 8. The length of the rod-shaped precipitates in alloy A2 increases while the density decreases as shown in Table 3. However for other dilute alloys, coarse precipitates with different morphologies were observed, replacing the needles-shaped precipitates.

Coarse precipitates present in alloy B2 were identified using TEM-EDX analyses. EDX analyses on coarse precipitate labelled as A as shown in Fig. 9 was suspected to be Mg_2Si. The Mg_2Si precipitate is the equilibrium stable phase in 6000 series alloys and always present in the over-aged alloys. This precipitate contributes little to the strength of 6000 series alloys [6]. In addition to the Mg_2Si precipitates, EDX analysis showed other coarse precipitates (labelled as B and C) such as Si and AlFeSi were also present in the alloys as observed in Figs. 10 and 11, respectively. However, it was very difficult to distinguish them from each other on the basis of their morphology.

4. Conclusions

Precipitation hardening behaviour in dilute 6000 series alloys with different Mg, Si and Cu content at different ageing temperature has been successfully investigated by TEM. It was found that the precipitates formed in the artificially aged alloys were mainly needle-shaped. The number density of precipitates increases as their solute content of Mg_2Si and ExSi increase. The addition of Cu (0.1 wt%) resulted in refinement of needle-shaped precipitates and may also have increased the number density of precipitates. The precipitation kinetics in the less dilute alloys is faster as compared to the more dilute alloys.

References

[1] D.E. Laughlin, W.F. Miao, Miner. Met. Mater. Soc. (1998) 63–79.
[2] M. Tamizifar, G.W. Lorimer, Proceedings of the 3rd International Conference on Aluminium Alloys, Trondheim: Norwegian Institute of Technology and Sintef Metallurgy, vol. l, 1992, pp. 220–225.
[3] D.G. Eskin, M.L. Kharakterova, Mater. Tehnol. 35 (1–2) (2001) 5–8.

[4] A.K. Gupta, D.J. Lloyd, S.A. Court, Mater. Sci. Eng. A 316 (2001) 11–17.
[5] L. Lodgaard, N. Ryum, Mater. Sci. Eng. A 283 (2000) 144–152.
[6] G.A. Edward, K. Stiller, G.L. Dunlop, M.J. Couper, Acta Mater. 46 (1998) 3893–3904.
[7] W.F. Miao, D.E. Laughlin, Scripta Mater. 40 (7) (1999) 873–878.
[8] W.F. Miao, D.E. Laughlin, Metall. Mater. Trans. A 31A (2000) 361–371.
[9] R.S. Yassar, D.P. Field, J. Mater. Res. 20 (2005) 2705–2711.
[10] C.D. Marioara, H. Nordmark, S.J. Andersen, J. Holmestad, J. Mater. Sci. 41 (2006) 471–478.
[11] G. Thomas, J. Inst. Met. 90 (1961–1962) 57–63.
[12] I. Dutta, S.M. Allen, J. Mater. Sci. Lett. 10 (1991) 323–326.
[13] M.H. Jacobs, Phil. Mag. 26 (1972) 1–13.
[14] P.M. Kelly, A. Jostsons, R.G. Blake, J.G. Napier, Phys. Status Solidi (a) 31 (2) (1975) 771–780.
[15] S. Esmaeili, X. Wang, D.J. Lloyd, W.J. Poole, Metall. Mater. Trans. A 34A (2003) 751–763.
[16] J.W. Martin, Precipitation Hardening, second ed., Butterworth-Heinemann, Oxford, 1998.
[17] M. Murayama, K. Hono, M. Saga, M. Kikuchi, Mater. Sci. Eng. A 250 (1998) 127–132.
[18] J.Y. Yao, D.A. Graham, B. Rinferer, M.J. Couper, Micron 32 (2001) 865–870.
[19] R.K. Wyss, L.W. Blazek, Mater. Sci. Forum 217–222 (1996) 1783–1788.
[20] D.J. Chakrabarti, D.E. Laughlin, Prog. Mater. Sci. 49 (2004) 389–410.
[21] M.A. Gaffar, A. Gaber, M.S. Mostafa, E. Abo Zeid, Mater. Sci. Eng. A 465 (2007) 274–282.
[22] J. Dutkiewicz, L. Litynska, Mater. Sci. Eng. A 324 (1–2) (2002) 239–243.
[23] A. Gaber, M.A. Gaffar, M.S. Mostafa, E.F.A. Zeid, J. Alloy Compd. 429 (1–2) (2006) 167–175.